ARL-TR-9590 • Sep 2022

DEVCOM ARMY RESEARCH LABORATORY

Largest Ellipsoid Estimation for Unknown Measurement Error Dynamics

by James Maley and Ryan Zurakowski

Approved for public release; distribution is unlimited.

NOTICES

Disclaimers

The findings in this report are not to be construed as an official Department of the Army position unless so designated by other authorized documents.

Citation of manufacturer's or trade names does not constitute an official endorsement or approval of the use thereof.

Destroy this report when it is no longer needed. Do not return it to the originator.

ARL-TR-9590 ● SEP 2022

Largest Ellipsoid Estimation for Unknown Measurement Error Dynamics

by James Maley
DEVCOM Army Research Laboratory

Ryan Zurakowski
Department of Biomedical Engineering, University of Delaware

Approved for public release; distribution is unlimited.

REPORT DOCUMENTATION PAGE

Form Approved
OMB No. 0704-0188

Public reporting burden for this collection of information is estimated to average 1 hour per response, including the time for reviewing instructions, searching existing data sources, gathering and maintaining the data needed, and completing and reviewing the collection information. Send comments regarding this burden estimate or any other aspect of this collection of information, including suggestions for reducing the burden, to Department of Defense, Washington Headquarters Services, Directorate for Information Operations and Reports (0704-0188), 1215 Jefferson Davis Highway, Suite 1204, Arlington, VA 22202-4302. Respondents should be aware that notwithstanding any other provision of law, no person shall be subject to any penalty for failing to comply with a collection of information if it does not display a currently valid OMB control number.

PLEASE DO NOT RETURN YOUR FORM TO THE ABOVE ADDRESS.

1. REPORT DATE *(DD-MM-YYYY)*	2. REPORT TYPE	3. DATES COVERED (From - To)
September 2022	Technical Report	January–July 2021

4. TITLE AND SUBTITLE
Largest Ellipsoid Estimation for Unknown Measurement Error Dynamics

5a. CONTRACT NUMBER

5b. GRANT NUMBER

5c. PROGRAM ELEMENT NUMBER

6. AUTHOR(S)
James Maley and Ryan Zurakowski

5d. PROJECT NUMBER
AH80

5e. TASK NUMBER

5f. WORK UNIT NUMBER

7. PERFORMING ORGANIZATION NAME(S) AND ADDRESS(ES)
DEVCOM Army Research Laboratory
ATTN: FCDD-RLW-WE
Aberdeen Proving Ground, MD 21005-5066

8. PERFORMING ORGANIZATION REPORT NUMBER
ARL-TR-9590

9. SPONSORING/MONITORING AGENCY NAME(S) AND ADDRESS(ES)

10. SPONSOR/MONITOR'S ACRONYM(S)

11. SPONSOR/MONITOR'S REPORT NUMBER(S)

12. DISTRIBUTION/AVAILABILITY STATEMENT
Approved for public release; distribution is unlimited.

13. SUPPLEMENTARY NOTES
primary author's email: <james.m.maley2.civ@army.mil>. ORCIDs: James Maley, 0000-0002-0861-9436, Ryan Zurakowski, 0000-0003-3726-3114

14. ABSTRACT
Largest ellipsoid estimation has promise for being able to handle measurement errors with known covariance but unknown dynamics. However, there is no proof that it will be consistent for a given system. The algorithm is converted into a covariance-form estimator, and the gain is clearly shown to be different from the Kalman gain. This formulation was used to examine the difference between the estimator covariance and the true covariance for the special case in which the measurement errors are constant. A counter-example shows that the estimator is not always consistent, but a consistency metric based on the steady-state covariance error is provided. Two simple simulation examples are used to demonstrate situations where the estimator works well and where it does not, while demonstrating the usefulness of the consistency metric.

15. SUBJECT TERMS
collaborative state estimation, information fusion, ellipsoid estimation, consistency metric, steady-state covariance, estimator

16. SECURITY CLASSIFICATION OF:			17. LIMITATION OF ABSTRACT	18. NUMBER OF PAGES	19a. NAME OF RESPONSIBLE PERSON
a. REPORT	b. ABSTRACT	c. THIS PAGE			James Maley
Unclassified	Unclassified	Unclassified	UU	30	19b. TELEPHONE NUMBER (Include area code) 410-306-1195

Standard Form 298 (Rev. 8/98)
Prescribed by ANSI Std. Z39.18

Contents

List of Figures iv

1. Introduction 1

2. Notation 3

3. Covariance-Form Largest Ellipsoid Estimator 3

4. Covariance Error Analysis 8

5. Consistency Metric 10

6. Example: Randomly Changing Disturbance 11

7. Example: Biased Sinewave Measurements 15

8. Conclusions 17

9. References 18

Appendix. Covariance Intersection Estimator 21

List of Acronyms 23

Distribution List 24

List of Figures

Fig. 1 States, estimates, and measurements for a sample run of the randomly changing disturbance example 12

Fig. 2 Estimation errors (black) along with estimator $\pm 3\sigma$ bounds (red) 13

Fig. 3 Average NEES comparison over 20 runs for randomly changing disturbance example 14

Fig. 4 Elements of the propagated LE covariance error (solid) and the most recent steady-state predictions (dashed) 14

Fig. 5 NEES comparisons for the biased sinewave example. Changing the ω from $0.1 \times 2\pi$ to $0.5 \times 2\pi$ changes the system enough to cause LE to become inconsistent. 16

Fig. 6 Elements of the propagated LE covariance error (solid) and the most recent steady-state predictions (dashed) for the biased sine wave example 16

1. Introduction

Estimating the states of a system requires accurate modeling of its propagation, outputs, and errors. Standard techniques based on Kalman filtering assume the errors afflicting the process and measurements are independent, identically distributed random variables with zero-mean and known covariance; often referred to as *noise*. This assumption is not always true, as in many cases, the errors are due to unmodeled deterministic processes, or possibly due to errors in the linearization of a nonlinear system. This leads to two similar kinds of problems: the unknown but bounded (UBB) disturbance problem from observer theory and the measurement fusion with unknown cross-correlation problem from distributed estimation theory. Both problems have solutions involving ellipsoids, which tend to be either computationally expensive or overly conservative. The present goal is to be able to design a simple, fast, and not-too-conservative estimator given the covariance of the measurement errors, without assuming anything about their dynamics or cross-correlations with the state estimation errors.

The UBB problem is often solved by so-called set-membership estimators. These compute a boundary in state space that defines the region where the state coordinates can feasibly reside. This idea started with Schweppe[1] and Witsenhausen.[2] Most set-membership estimators use an ellipsoid to approximate the set boundary,[3] although other geometrical constructs have been used. Calafiore[4] estimated an optimal bounding ellipsoid subject to a linear matrix inequality constraint by solving a semidefinite programming problem at each prediction and update step. This idea has been expanded on since then with robust cost functions.[5–8] The disadvantage of these approaches is the complexity of repeatedly solving the optimizations. The linear matrix inequality problems can sometimes be solved prior to running the observer, but only for a subset of systems such as linear time invariant (LTI) systems[9] or linear parameter varying systems.[10] Some algorithms instead use a convex combination of covariance ellipsoids in the propagation step and convex combinations of information ellipsoids in the update step[11,12] (although with different terminology). These methods are simpler, but can be too conservative.

Some distributed estimation problems solve a similar problem to the UBB disturbance one, in which measurements must be used that have errors that may or may not be correlated with the current state errors. The baseline tool for fusing possibly

correlated information is the covariance intersection (CI) algorithm,[13] which also uses a convex combination of information matrices to find the fused information matrix. The reason the UBB problem is similar is that once a measurement with UBB errors is used to update a state estimate, future measurements cannot be assumed to be uncorrelated with the state estimation errors. The ellipsoids represent covariance (or information) matrices instead of set boundaries, but the goal is still to make the ellipsoid maintained by the filter contain the true ellipsoid. Covariance intersection is readily adapted to situations where some of the information being fused is known to be uncorrelated with something call split-covariance intersection,[14] but even with this extra information, it is sometimes too conservative to be of practical use.

Less-conservative alternatives to CI include robust fusion,[15] inverse covariance intersection,[16] and largest ellipsoid (LE) estimation.[17] Of these, the least conservative and complex is largest ellipsoid intersection, which (with minor differences) has also been called SAFE fusion[18] or ellipsoidal intersection (EI).[19] In contrast to a convex sum of information matrices used by CI, the LE update computes the minimum volume ellipsoid that contains both the prior and measurement information ellipsoids.[20] LE estimation has been demonstrated to be consistent in track-to-track fusion problems[21] or for fusing nonlinear state estimates from multiple estimators.[22] The problem is that even though LE estimation is often consistent in practice, consistency is not guaranteed[23] except in a few special cases. In the original formulation of EI by Sijs,[19] the two estimates to be fused are assumed to be the optimal combination of a common prior estimate with two independent information sources. Forsling[20] restricts LE use to when the joint covariance from the two measurements to be fuse has a component-wise aligned structure. This means that if a transformation can diagonalize both measurement covariance matrices, the resulting transformed cross-correlation matrices are also diagonal.

Because of its simplicity and accuracy, LE estimation has promise as either a statistical or UBB state estimator, although it has not been widely applied to state estimation problems with indirect measurements. First, the information-form estimator described in Forsling[20] is expanded on to provide a covariance-form estimator, which is then compared to a Kalman filter. Our results contradict the result at the end of Noack et al.[24] stating that the LE fusion gains are identical to the Bar-Shalom/Campo gains. Possibly correlated propagation noise is not addressed here;

only the case of possibly correlated measurement noise. To address the consistency issue, a special case is examined in which the measurement errors are random constants (unbeknownst to the estimator), but with a known covariance. Clearly, this leads to cross-correlation between the state errors and measurement errors. Analysis of the covariance-form LE estimator shows that by the second update we can no longer say that the estimated covariance fully contains the true covariance (the difference is not positive semi-definite). However, we then produce recursion relationships for the error between the true and estimated covariance matrices. This can be used to forecast what the steady-state covariance error will be, which can be used as a consistency metric.

2. Notation

Matrices are written as bold uppercase and vectors with bold lowercase symbols. The transpose operator is denoted $\mathbf{X}^\top$, while the inverse of the transpose is denoted $\mathbf{X}^{-\top}$. Mean vectors and covariance matrices maintained by the estimator are denoted $\hat{\mathbf{x}},\ \hat{\mathbf{X}}$, while the errors are denoted by $\tilde{\mathbf{x}} = \mathbf{x} - \hat{\mathbf{x}},\ \tilde{\mathbf{X}} = \mathbf{X} - \hat{\mathbf{X}}$. The identity matrix is always $\mathbf{I}$. Subscript k denotes the values at that timestamp, subscript $k|k-1$ is used to denote quantities after the propagation step, but before the update step of the estimator, and subscript $k|m$ is used to denote information from measurements. Expectations are denoted $\mathrm{E}[\dots]$ and $\mathbf{v} \sim \mathcal{N}(\boldsymbol{\mu}, \mathbf{C})$ indicates the vector $\mathbf{v}$ is normally distributed with mean $\boldsymbol{\mu}$ and covariance $\mathbf{C}$. The covariance shortcut $\mathrm{Cov}(\mathbf{x}) = \mathrm{E}\left[(\mathbf{x} - \mathrm{E}[\mathbf{x}])(\mathbf{x} - \mathrm{E}[\mathbf{x}])^\top\right]$ is used. The matrix inequality $\mathbf{M}_1 \succeq \mathbf{M}_2$ indicates that $\mathbf{M}_1 - \mathbf{M}_2$ is positive semidefinite. The operation $\boldsymbol{\Lambda}^{-d}$ only works on diagonal matrices $\boldsymbol{\Lambda} = diag(d_1, d_2, \dots, 0, 0)$ so that each diagonal element in d_i becomes $1/d_i$ unless $d_i = 0$, so that $\boldsymbol{\Lambda}^{-d} = diag(1/d_1, 1/d_2, \dots, 0, 0)$.

3. Covariance-Form Largest Ellipsoid Estimator

Consider the LTI discrete-time system defined by

$$\mathbf{x}_k = \mathbf{F}\mathbf{x}_{k-1} + \mathbf{L}\mathbf{u}_k + \mathbf{w}_{k-1} \tag{1}$$

$$\mathbf{m}_k = \mathbf{H}\mathbf{x}_k + \mathbf{G}\mathbf{y}_k \tag{2}$$

where the $\mathbf{x}_k$ is the true state of the system, $\mathbf{u}_k$ is the known input, $\mathbf{w}_k \sim \mathcal{N}(\mathbf{0}, \mathbf{Q})$ is the process noise, and $\mathbf{m}_k$ are the measurements that are affected by a zero-mean disturbance vector $\mathbf{y}_k$. The estimator maintains an estimate of the state $\hat{\mathbf{x}}$, as well

as an estimate of the error covariance $\hat{\mathbf{X}}$, which is not necessarily the same as the true error covariance $\mathrm{Cov}\left(\hat{\mathbf{x}}\right) = \mathbf{X}$. The estimator has a predictor step

$$\hat{\mathbf{x}}_{k|k-1} = \mathbf{F}\hat{\mathbf{x}}_{k-1} + \mathbf{L}\mathbf{u}_k \tag{3}$$

$$\hat{\mathbf{X}}_{k|k-1} = \mathbf{F}\hat{\mathbf{X}}_k\mathbf{F}^\top + \mathbf{Q} \tag{4}$$

and a corrector step

$$\hat{\mathbf{x}}_k = \hat{\mathbf{x}}_{k|k-1} - \mathbf{K}_k\mathbf{H}\hat{\mathbf{x}}_{k|k-1} + \mathbf{K}_k\mathbf{m}_k \tag{5}$$

$$\hat{\mathbf{X}}_k = \left(\mathbf{I} - \mathbf{K}_k\mathbf{H}\right)\hat{\mathbf{X}}_{k|k-1}\left(\mathbf{I} - \mathbf{K}_k\mathbf{H}\right)^\top + \mathbf{K}\mathbf{M}\mathbf{K}^\top, \tag{6}$$

where $\mathbf{M} = \mathbf{G}\mathbf{Y}\mathbf{G}^\top$. The estimator error is correlated with the disturbance vector:

$$\mathrm{Cov}\left(\begin{bmatrix}\tilde{\mathbf{x}}_{k|k-1}\\ \mathbf{y}_k\end{bmatrix}\right) = \begin{bmatrix}\mathbf{X}_{k|k-1} & \mathbf{\Sigma}_{k|k-1}\\ \mathbf{\Sigma}_{k|k-1}^\top & \mathbf{Y}_k\end{bmatrix} \tag{7}$$

$$\mathrm{Cov}\left(\begin{bmatrix}\tilde{\mathbf{x}}_k\\ \mathbf{y}_k\end{bmatrix}\right) = \begin{bmatrix}\mathbf{X}_k & \mathbf{\Sigma}_k\\ \mathbf{\Sigma}_k^\top & \mathbf{Y}_k\end{bmatrix} \tag{8}$$

The gain matrix $\mathbf{K}_k$ is a function of the estimated error covariance $\hat{\mathbf{X}}_{k|k-1}$ and $\mathbf{Y}_k$, but $\mathbf{\Sigma}_k$ is unknown. The well-known Kalman gain $\mathbf{K}_k^* = \hat{\mathbf{X}}_{k|k-1}\mathbf{H}^\top\left(\mathbf{H}\hat{\mathbf{X}}_{k|k-1}\mathbf{H}^\top + \mathbf{M}\right)^{-1}$ is optimal if $\mathbf{\Sigma}_k = \mathbf{0}$. The corrector step (5–6) can also be written in terms of information matrices

$$\hat{\boldsymbol{\mathcal{I}}}_{k|k-1} = \hat{\mathbf{X}}_{k|k-1}^{-1} \qquad\qquad \boldsymbol{\mathcal{I}}_{k|m} = \mathbf{H}^\top\mathbf{M}^{-1}\mathbf{H} \tag{9}$$

and information vectors

$$\hat{\boldsymbol{\iota}}_{k|k-1} = \hat{\mathbf{X}}_{k|k-1}^{-1}\hat{\mathbf{x}}_{k|k-1} \tag{10}$$

$$\boldsymbol{\iota}_{k|m} = \mathbf{H}^\top\mathbf{M}^{-1}\mathbf{m}. \tag{11}$$

Using the Kalman gain results in simple summations:

$$\hat{\boldsymbol{\iota}}_k^* = \hat{\boldsymbol{\iota}}_{k|k-1} + \boldsymbol{\iota}_{k|m} \qquad\qquad \hat{\boldsymbol{\mathcal{I}}}_k^* = \hat{\boldsymbol{\mathcal{I}}}_{k|k-1} + \boldsymbol{\mathcal{I}}_{k|m} \tag{12}$$

This is the well-known "information-form" of the Kalman filter. For LE estimation, instead of a summation, the updated information matrix represents the minimal volume ellipsoid containing the ellipsoids represented by $\hat{\boldsymbol{\mathcal{I}}}_{k|k-1}$ and $\boldsymbol{\mathcal{I}}_{k|m}$. A joint

diagonalization transformation $\mathbf{T}_k$ is computed so that

$$\mathbf{T}_k \hat{\boldsymbol{\mathcal{I}}}_{k|k-1} \mathbf{T}_k^\top = \mathbf{I} \qquad \hat{\boldsymbol{\iota}}'_{k|k-1} = \mathbf{T}_k \hat{\boldsymbol{\iota}}_{k|k-1} \tag{13}$$

$$\mathbf{T}_k \hat{\boldsymbol{\mathcal{I}}}_{k|m} \mathbf{T}_k^\top = \boldsymbol{\Lambda}_k \qquad \boldsymbol{\iota}'_{k|m} = \mathbf{T}_k \boldsymbol{\iota}_{k|m}. \tag{14}$$

where $\boldsymbol{\Lambda}_k$ is diagonal. The transformed, updated information vector and matrix are chosen element-wise based on the largest value of the transformed information matrices. That is,

$$\hat{\boldsymbol{\mathcal{I}}}'_k = \mathbf{A}_k + \mathbf{B}_k \boldsymbol{\Lambda}_k, \qquad \hat{\boldsymbol{\iota}}'_k = \mathbf{A}_k \hat{\boldsymbol{\iota}}'_{k|k-1} + \mathbf{B}_k \boldsymbol{\iota}'_{k|m} \tag{15}$$

where $\mathbf{B}_k$ is a diagonal matrix with the i'th component $\mathbf{B}_k[i,i] = 1$ if $\boldsymbol{\Lambda}_k[i,i] > 1$, and $\mathbf{B}_k[i,i] = 0$ otherwise. The matrix $\mathbf{A}_k$ is the opposite so that

$$\mathbf{A}_k + \mathbf{B}_k = \mathbf{I}, \qquad \mathbf{A}_k \mathbf{B}_k = \mathbf{0}. \tag{16}$$

The updated information vector and matrix are given by

$$\hat{\boldsymbol{\mathcal{I}}}_k = \mathbf{T}_k^{-1} \hat{\boldsymbol{\mathcal{I}}}'_k \mathbf{T}_k^{-\top} \qquad \hat{\boldsymbol{\iota}}_k = \mathbf{T}_k^{-1} \hat{\boldsymbol{\iota}}'_k, \tag{17}$$

which can be transformed back into the state vector and covariance matrix by

$$\hat{\mathbf{X}}_k = \hat{\boldsymbol{\mathcal{I}}}_k^{-1} \qquad \hat{\mathbf{x}}_k = \hat{\boldsymbol{\mathcal{I}}}_k^{-1} \hat{\boldsymbol{\iota}}_k \tag{18}$$

The transformation $\mathbf{T}_k$ can be directly computed through the following singular value decompositions (SVDs):

$$\mathbf{U}\mathbf{D}\mathbf{U}^\top = \hat{\boldsymbol{\mathcal{I}}}_{k|k-1} \tag{19}$$

$$\mathbf{V}\boldsymbol{\Lambda}_k\mathbf{V}^\top = \left(\mathbf{D}^{-1/2}\mathbf{U}^\top\right) \boldsymbol{\mathcal{I}}_{k|m} \left(\mathbf{D}^{-1/2}\mathbf{U}^\top\right)^\top \tag{20}$$

$$\mathbf{T}_k = \mathbf{V}^\top \mathbf{D}^{-1/2} \mathbf{U}^\top, \tag{21}$$

where $\mathbf{D}$ and $\boldsymbol{\Lambda}_k$ are diagonal, and $\mathbf{U}$ and $\mathbf{V}$ are orthonormal. Note that this formulation assumes $\hat{\mathbf{X}}_{k|k-1}$ is full rank, but not $\mathbf{H}^\top \mathbf{M}^{-1} \mathbf{H}$.

Equations 9–21 describe the basic algorithm in Forsling,[20] just slightly more tailored to the state estimation problem. We now wish to describe the estimator in a "covariance-form" to make it easier to implement and analyze. To start, the SVD in

Eq. 19 can be computed on $\hat{\mathbf{X}}_{k|k-1}$ instead of $\hat{\mathbf{X}}^{-1}_{k|k-1}$, since

$$\hat{\mathbf{X}}_{k|k-1} = \hat{\boldsymbol{\mathcal{I}}}^{-1}_{k|k-1} = \mathbf{U}\mathbf{D}^{-1}\mathbf{U}^{\top}. \tag{22}$$

Combining Eqs. 15, 17, and 18 with some algebra leads to

$$\hat{\mathbf{X}}_k = \mathbf{T}_k^{\top}\left(\mathbf{A}_k + \mathbf{B}_k\boldsymbol{\Lambda}_k\right)^{-1}\mathbf{T}_k. \tag{23}$$

Because each diagonal element in the sum $\mathbf{A}_k + \mathbf{B}_k\boldsymbol{\Lambda}_k$ is either 1 or the element of $\boldsymbol{\Lambda}_k$, the $\boldsymbol{\Lambda}_k^{-d}$ operator defined in the notation section can be applied to get

$$\hat{\mathbf{X}}_k = \mathbf{T}_k^{\top}\left(\mathbf{A}_k + \mathbf{B}_k\boldsymbol{\Lambda}_k^{-d}\right)\mathbf{T}_k. \tag{24}$$

With the same substitutions, the updated state vector leads to

$$\hat{\mathbf{x}}_k = \mathbf{T}_k^{\top}\left(\mathbf{A}_k + \mathbf{B}_k\boldsymbol{\Lambda}_k^{-d}\right)\left(\mathbf{A}_k\hat{\boldsymbol{\iota}}'_{k|k-1} + \mathbf{B}_k\boldsymbol{\iota}'_{k|m}\right) \tag{25}$$

Acknowledging that because $\boldsymbol{\Lambda}_k$ is diagonal, $\mathbf{B}_k\boldsymbol{\Lambda}_k^{-d}\mathbf{A}_k$ is $\mathbf{0}$ and substituting in the information vector definitions leads to

$$\begin{aligned}\hat{\mathbf{x}}_k = {} & \mathbf{T}_k^{\top}\mathbf{A}_k\mathbf{T}_k\hat{\mathbf{X}}^{-1}_{k|k-1}\hat{\mathbf{x}}_{k|k-1} \\ & \cdots + \mathbf{T}_k^{\top}\mathbf{B}_k\boldsymbol{\Lambda}_k^{-d}\mathbf{T}_k\mathbf{H}^{\top}\mathbf{M}^{-1}\mathbf{m}\end{aligned} \tag{26}$$

Substituting the information matrix definitions into Eq. 13 leads to

$$\mathbf{T}_k\hat{\mathbf{X}}^{-1}_{k|k-1}\mathbf{T}_k^{\top} = \mathbf{I} \tag{27}$$

$$\mathbf{T}_k\hat{\mathbf{X}}^{-1}_{k|k-1} = \mathbf{T}_k^{-\top}. \tag{28}$$

With this, the state update becomes

$$\hat{\mathbf{x}}_k = \mathbf{T}_k^{\top}\mathbf{A}_k\mathbf{T}_k^{-\top}\hat{\mathbf{x}}_{k|k-1} + \mathbf{T}_k^{\top}\mathbf{B}_k\boldsymbol{\Lambda}_k^{-d}\mathbf{T}_k\mathbf{H}^{\top}\mathbf{M}^{-1}\mathbf{m}$$

From this, the LE estimator gain terms from Eq. 5 are

$$\mathbf{K}_k = \mathbf{T}_k^{\top}\mathbf{B}_k\boldsymbol{\Lambda}_k^{-d}\mathbf{T}_k\mathbf{H}^{\top}\mathbf{M}^{-1} \tag{29}$$

$$\mathbf{I} - \mathbf{K}_k\mathbf{H} = \mathbf{T}_k^{\top}\mathbf{A}_k\mathbf{T}_k^{-\top}. \tag{30}$$

The optimal Kalman gain can also be computed using the transformed information matrices. Starting from Eq. 12

$$\hat{\boldsymbol{\mathcal{I}}}_k^* = \mathbf{T}_k^{-1}\mathbf{T}_k \left(\hat{\boldsymbol{\mathcal{I}}}_{k|k-1} + \boldsymbol{\mathcal{I}}_{k|m}\right) \mathbf{T}_k^\top \mathbf{T}_k^{-\top} \tag{31}$$

$$= \mathbf{T}_k^{-1} \left(\mathbf{I} + \boldsymbol{\Lambda}_k\right) \mathbf{T}_k^{-\top} \tag{32}$$

$$\hat{\mathbf{X}}_k^* = \mathbf{T}_k^\top \left(\mathbf{I} + \boldsymbol{\Lambda}_k\right)^{-1} \mathbf{T}_k \tag{33}$$

$$\hat{\mathbf{x}}_k^* = \hat{\boldsymbol{\mathcal{I}}}_k^{*-1} \left(\hat{\boldsymbol{\imath}}_{k|k-1} + \boldsymbol{\imath}_{k|m}\right) \tag{34}$$

$$= \mathbf{T}_k^\top \left(\mathbf{I} + \boldsymbol{\Lambda}_k\right)^{-1} \mathbf{T}_k^{-\top} \hat{\mathbf{x}}_{k|k-1} + \mathbf{T}_k^\top \left(\mathbf{I} + \boldsymbol{\Lambda}_k\right)^{-1} \mathbf{T}_k \mathbf{H}^\top \mathbf{M}^{-1} \mathbf{m}. \tag{35}$$

So, the Kalman gain terms are

$$\mathbf{K}_k^* = \mathbf{T}_k^\top \left(\mathbf{I} + \boldsymbol{\Lambda}_k\right)^{-1} \mathbf{T}_k \mathbf{H}^\top \mathbf{M}^{-1} \tag{36}$$

$$\mathbf{I} - \mathbf{K}_k^* \mathbf{H} = \mathbf{T}_k^\top \left(\mathbf{I} + \boldsymbol{\Lambda}_k\right)^{-1} \mathbf{T}_k^{-\top}. \tag{37}$$

Note that the optimal information fusion in Bar Shalom/Campo[25] is algebraically equivalent to a Kalman filter update when $\mathbf{H} = \mathbf{G} = \mathbf{I}$. With this simplification

$$\mathbf{T}_k \hat{\boldsymbol{\mathcal{I}}}_{k|m} \mathbf{T}_k^\top \implies \mathbf{T}_k \mathbf{Y}^{-1} \mathbf{T}_k^\top = \boldsymbol{\Lambda}_k \tag{38}$$

$$\mathbf{T}_k \mathbf{H}^\top \mathbf{M}^{-1} \implies \mathbf{T}_k \mathbf{Y}^{-1} = \boldsymbol{\Lambda}_k \mathbf{T}_k^{-\top} \tag{39}$$

Substituting Eq. 39 into Eq. 29 gives $\mathbf{K}_k = \mathbf{T}_k^\top \mathbf{B}_k \mathbf{T}_k^{-\top}$, while substituting it into Eq. 36 gives $\mathbf{K}_k^* = \mathbf{T}_k^\top \left(\mathbf{I} + \boldsymbol{\Lambda}_k\right)^{-1} \boldsymbol{\Lambda}_k \mathbf{T}_k^{-\top}$. Although the largest ellipsoid gain has similar behavior to the optimal gain, it is not identical, which contradicts the assertion made in Theorem 4 of Noack et al.[24] that it should be.

4. Covariance Error Analysis

The goal of distributed estimation problems or UBB problems is to have $\hat{\mathbf{X}} \succeq \mathbf{X}$. We restrict the analysis here to the case when $\mathbf{y}_k = \mathbf{y}_{k-1}$. Because $\mathbf{Y}$ is constant, it will be subscript-less. The joint error covariance therefore propagates according to

$$\begin{bmatrix} \mathbf{X}_{k|k-1} & \mathbf{\Sigma}_{k|k-1} \\ \mathbf{\Sigma}_{k|k-1}^\top & \mathbf{Y} \end{bmatrix} = \begin{bmatrix} \mathbf{F} & \mathbf{0} \\ \mathbf{0} & \mathbf{I} \end{bmatrix} \begin{bmatrix} \mathbf{X}_{k-1} & \mathbf{\Sigma}_{k-1} \\ \mathbf{\Sigma}_{k-1}^\top & \mathbf{Y} \end{bmatrix} \begin{bmatrix} \mathbf{F}^\top & \mathbf{0} \\ \mathbf{0} & \mathbf{I} \end{bmatrix} + \begin{bmatrix} \mathbf{Q} & \mathbf{0} \\ \mathbf{0} & \mathbf{0} \end{bmatrix}^\top$$

so that

$$\mathbf{X}_{k|k-1} = \mathbf{F}\mathbf{X}_{k-1}\mathbf{F}^\top + \mathbf{Q} \tag{40}$$

$$\mathbf{\Sigma}_{k|k-1} = \mathbf{F}\mathbf{\Sigma}_{k-1} \tag{41}$$

After the update step, the joint error covariance becomes

$$\begin{bmatrix} \mathbf{X}_k & \mathbf{\Sigma}_k \\ \mathbf{\Sigma}_k^\top & \mathbf{Y} \end{bmatrix} = \begin{bmatrix} (\mathbf{I} - \mathbf{K}_k\mathbf{H}) & -\mathbf{K}_k\mathbf{G} \\ \mathbf{0} & \mathbf{I} \end{bmatrix} \begin{bmatrix} \mathbf{X}_{k|k-1} & \mathbf{\Sigma}_{k|k-1} \\ \mathbf{\Sigma}_{k|k-1}^\top & \mathbf{Y} \end{bmatrix} \begin{bmatrix} (\mathbf{I} - \mathbf{H}_k^\top\mathbf{K}^\top) & \mathbf{0} \\ -\mathbf{G}^\top\mathbf{K}_k^\top & \mathbf{I} \end{bmatrix} \tag{42}$$

so that

$$\begin{aligned} \mathbf{X}_k = &(\mathbf{I} - \mathbf{K}_k\mathbf{H})\,\mathbf{X}_{k|k-1}\,(\mathbf{I} - \mathbf{K}_k\mathbf{H})^\top \\ &\cdots - (\mathbf{I} - \mathbf{K}_k\mathbf{H})\,\mathbf{\Sigma}_{k|k-1}\mathbf{G}^\top\mathbf{K}_k^\top \\ &\cdots - \mathbf{K}_k\mathbf{G}\mathbf{\Sigma}_{k|k-1}^\top\,(\mathbf{I} - \mathbf{K}_k\mathbf{H})^\top + \mathbf{K}_k\mathbf{M}\mathbf{K}_k^\top \end{aligned} \tag{43}$$

$$\mathbf{\Sigma}_k = (\mathbf{I} - \mathbf{K}_k\mathbf{H})\,\mathbf{\Sigma}_{k|k-1} - \mathbf{K}_k\mathbf{G}\mathbf{Y} \tag{44}$$

The recursion for computing the covariance error $\tilde{\mathbf{X}} = \mathbf{X} - \hat{\mathbf{X}}$ is useful for examining consistency. Combining Eqs. 40 and 4 gives

$$\tilde{\mathbf{X}}_{k|k-1} = \mathbf{F}\tilde{\mathbf{X}}_{k-1}\mathbf{F}^\top. \tag{45}$$

Combining Eq. 43 with Eq. 6 leads to

$$\begin{aligned} \tilde{\mathbf{X}}_k = &(\mathbf{I} - \mathbf{K}_k\mathbf{H})\,\tilde{\mathbf{X}}_{k|k-1}\,(\mathbf{I} - \mathbf{K}_k\mathbf{H})^\top \\ &\cdots - (\mathbf{I} - \mathbf{K}_k\mathbf{H})\,\mathbf{\Sigma}_{k|k-1}\mathbf{G}^\top\mathbf{K}_k^\top \\ &\cdots - \mathbf{K}_k\mathbf{G}\mathbf{\Sigma}_{k|k-1}^\top\,(\mathbf{I} - \mathbf{K}_k\mathbf{H})^\top \end{aligned} \tag{46}$$

Combining the propagation and update steps, along with Eq. 41 leads to

$$\begin{aligned}\tilde{\mathbf{X}}_k = &\left(\mathbf{I} - \mathbf{K}_k\mathbf{H}\right)\mathbf{F}\tilde{\mathbf{X}}_{k-1}\mathbf{F}^\top\left(\mathbf{I} - \mathbf{K}_k\mathbf{H}\right)^\top \\ &\cdots - \left(\mathbf{I} - \mathbf{K}_k\mathbf{H}\right)\mathbf{F}\boldsymbol{\Sigma}_{k-1}\mathbf{G}^\top\mathbf{K}_k^\top \\ &\cdots - \mathbf{K}_k\mathbf{G}\boldsymbol{\Sigma}_{k-1}^\top\mathbf{F}^\top\left(\mathbf{I} - \mathbf{K}_k\mathbf{H}\right)^\top \end{aligned} \tag{47}$$

while combining Eqs. 40 and 44 leads to

$$\boldsymbol{\Sigma}_k = \left(\mathbf{I} - \mathbf{K}_k\mathbf{H}\right)\mathbf{F}\boldsymbol{\Sigma}_{k-1} - \mathbf{K}_k\mathbf{G}\mathbf{Y}. \tag{48}$$

Suppose that under ideal circumstances the estimator is initialized consistently and independently of the disturbance so that $\tilde{\mathbf{X}}_0 = \mathbf{0}$ and $\boldsymbol{\Sigma}_0 = \mathbf{0}$. From Eq. 47, at $k = 1$, $\tilde{\mathbf{X}}_1 = \mathbf{0}$ still but from Eq. 48 $\boldsymbol{\Sigma}_1 = -\mathbf{K}_1\mathbf{G}\mathbf{Y}$. So, by the time $k = 2$, the covariance error is in general nonzero:

$$\tilde{\mathbf{X}}_2 = \left(\mathbf{I} - \mathbf{K}_2\mathbf{H}\right)\mathbf{F}\mathbf{K}_1\mathbf{G}\mathbf{Y}\mathbf{G}^\top\mathbf{K}_2^\top + \mathbf{K}_2\mathbf{G}\mathbf{Y}\mathbf{G}^\top\mathbf{K}_1^\top\mathbf{F}^\top\left(\mathbf{I} - \mathbf{K}_2\mathbf{H}\right)^\top \tag{49}$$

Examining one of the terms in the above summation with the definition of the Kalman gain leads to

$$\begin{aligned}&\left(\mathbf{I} - \mathbf{K}_2\mathbf{H}\right)\mathbf{F}\mathbf{K}_1\mathbf{G}\mathbf{Y}\mathbf{G}^\top\mathbf{K}_2^\top \ldots \\ &= \mathbf{T}_2^\top\mathbf{A}_2\mathbf{T}_2^{-\top}\mathbf{F}\mathbf{K}_1\mathbf{M}\mathbf{K}_2^\top &(50)\\ &= \mathbf{T}_2^\top\mathbf{A}_2\mathbf{T}_2^{-\top}\mathbf{F}\mathbf{T}_1^\top\mathbf{B}_1\boldsymbol{\Lambda}_1^{-d}\mathbf{T}_1\mathbf{H}^\top\mathbf{M}^{-1}\mathbf{H}\mathbf{T}_2^\top\boldsymbol{\Lambda}_2^{-d}\mathbf{B}_2\mathbf{T}_2 &(51)\end{aligned}$$

There are a number of conditions that *could* cause $\tilde{\mathbf{X}}_2$ to be $\mathbf{0}$; however, a consistency proof would require showing that $\tilde{\mathbf{X}}_2$ is negative semi-definite. This is not the case if $\mathbf{B}_2 \neq \mathbf{0}$ and $\mathbf{A}_2 \neq \mathbf{0}$. The term in Eq. 51 can be rewritten

$$\left(\mathbf{I} - \mathbf{K}_2\mathbf{H}\right)\mathbf{F}\mathbf{K}_1\mathbf{G}\mathbf{Y}\mathbf{G}^\top\mathbf{K}_2^\top = \mathbf{T}_2^\top\mathbf{A}_2\boldsymbol{\psi}\mathbf{B}_2\mathbf{T}_2 \tag{52}$$

and the $\mathbf{A}_2\boldsymbol{\psi}\mathbf{B}_2$ matrix will have zeros on the diagonal. To see this, consider the case in which the diagonal elements in $\boldsymbol{\Lambda}_2$ are arranged in descending order. This means

$$\mathbf{A}_2\boldsymbol{\psi}\mathbf{B}_2 = \begin{bmatrix} \mathbf{0} & \mathbf{0} \\ \mathbf{0} & \mathbf{I} \end{bmatrix} \begin{bmatrix} \boldsymbol{\psi}_{11} & \boldsymbol{\psi}_{12} \\ \boldsymbol{\psi}_{21} & \boldsymbol{\psi}_{22} \end{bmatrix} \begin{bmatrix} \mathbf{I} & \mathbf{0} \\ \mathbf{0} & \mathbf{0} \end{bmatrix} \tag{53}$$

$$= \begin{bmatrix} \mathbf{0} & \mathbf{0} \\ \boldsymbol{\psi}_{21} & \mathbf{0} \end{bmatrix} \tag{54}$$

Using this result in Eq. 49 yields

$$\tilde{\mathbf{X}}_2 = \mathbf{T}_2^\top \begin{bmatrix} \mathbf{0} & \boldsymbol{\psi}_{21}^\top \\ \boldsymbol{\psi}_{21} & \mathbf{0} \end{bmatrix} \mathbf{T}_2, \tag{55}$$

which is neither positive nor negative semi-definite.

5. Consistency Metric

A major problem with LE estimation is if it becomes inconsistent, there is no way to know during runtime. There also is not a metric for even simple LTI systems that can tell the designer if the LE estimator will be consistent. However, it is possible that in the case where the estimator covariance reaches a steady-state value, we can examine the steady-state value of $\tilde{\mathbf{X}}$. Steady-state values will be indicated by subscript $k = \infty$. If the value of $\hat{\mathbf{X}}_\infty$ is known, then the steady-state estimator gain $\mathbf{K}_\infty$ can be computed from Eqs. 19, 20, 21, and 29. The steady-state cross-correlation can be computed by solving Eq. 48:

$$\boldsymbol{\Sigma}_\infty = (\mathbf{I} - \mathbf{K}_\infty\mathbf{H})\,\mathbf{F}\boldsymbol{\Sigma}_\infty - \mathbf{K}_\infty\mathbf{G}\mathbf{Y} \tag{56}$$

$$\boldsymbol{\Sigma}_\infty = -\left(\mathbf{I} - (\mathbf{I} - \mathbf{K}_\infty\mathbf{H})\,\mathbf{F}\right)^{-1}\mathbf{K}_\infty\mathbf{G}\mathbf{Y} \tag{57}$$

Then $\tilde{\mathbf{X}}_\infty$ results from Eq. 47, which becomes a discrete Lyapunov equation:

$$\begin{aligned} \mathbf{0} = {} & (\mathbf{I} - \mathbf{K}_k\mathbf{H})\,\mathbf{F}\tilde{\mathbf{X}}_\infty\mathbf{F}^\top\,(\mathbf{I} - \mathbf{K}_\infty\mathbf{H})^\top \\ & \cdots - \tilde{\mathbf{X}}_\infty \\ & \cdots - (\mathbf{I} - \mathbf{K}_\infty\mathbf{H})\,\mathbf{F}\boldsymbol{\Sigma}_\infty\mathbf{G}^\top\mathbf{K}_\infty^\top \\ & \cdots - \mathbf{K}_\infty\mathbf{G}\boldsymbol{\Sigma}_\infty^\top\mathbf{F}^\top\,(\mathbf{I} - \mathbf{K}_\infty\mathbf{H})^\top \end{aligned} \tag{58}$$

From here, $\tilde{\mathbf{X}}_\infty$ can be checked to see if the diagonal elements are ≤ 0, which is a less-restrictive condition than showing that $\tilde{\mathbf{X}}_\infty$ is negative semi-definite. This indicates that $\hat{\mathbf{X}}$ is at least "trace consistent" (i.e., tr $\left(\hat{\mathbf{X}}_\infty\right) \geq$ tr $(\mathbf{X}_\infty)$ as in Leonardos and Daniilidis[15]). The primary problem with this check is that $\hat{\mathbf{X}}_\infty$ cannot be computed from a discrete algebraic Riccati equation like it is possible to do with a Kalman filter. In fact, no explicit solution for $\hat{\mathbf{X}}_\infty$ is presented here. However, it is still possible to use the current value of $\hat{\mathbf{X}}_k$ in the place of $\hat{\mathbf{X}}_\infty$, as this will likely reach the steady-state value and is readily available. The conjecture that an estimator covariance for a detectable LTI system will reach a steady-state has not been proven when using LE estimation. Care must also be taken because the calculations do not work when $\mathbf{K}_k = \mathbf{0}$.

A secondary problem with this check is that it is only exact for the case when the disturbance is constant. However, in practice, this is still a useful metric as is demonstrated in the following examples.

6. Example: Randomly Changing Disturbance

Consider the state-space model for a randomly driven constant acceleration model with position p, velocity v, and acceleration a:

$$\begin{bmatrix} \dot{p} \\ \dot{v} \\ \dot{a} \end{bmatrix} = \begin{bmatrix} 0 & 1 & 0 \\ 0 & 0 & 1 \\ 0 & 0 & 0 \end{bmatrix} \begin{bmatrix} p \\ v \\ a \end{bmatrix} + \begin{bmatrix} 0 & 0 & 0 \\ 0 & 0 & 0 \\ 0.01 & 1 & 1 \end{bmatrix} \begin{bmatrix} 100 - \hat{p} \\ 0 - \hat{v} \\ 0 - \hat{a} \end{bmatrix} + \begin{bmatrix} 0 \\ 0 \\ w_3 \end{bmatrix}, \tag{59}$$

where w_3 is an independent unit white noise process. The inputs are the error between set points and the estimated states. The system is discretized (see Section 4.2 of Simon[26]) with a timestep of 0.1. At each timestep, the disturbance d has a 1% chance to obtain a new value drawn from $\mathcal{N}(0, 100)$. This creates errors with a known covariance, but not a known time correlation. The measurement equation is

$$m = \underbrace{\begin{bmatrix} 1 & 0 & 0 \end{bmatrix}}_{\mathbf{H}} \underbrace{\begin{bmatrix} p \\ v \\ a \end{bmatrix}}_{\mathbf{x}} + \underbrace{\begin{bmatrix} 1 \end{bmatrix}}_{\mathbf{G}} \underbrace{\begin{bmatrix} d \end{bmatrix}}_{\mathbf{y}}. \tag{60}$$

An example MATLAB[27] simulation run is shown in Fig. 1.

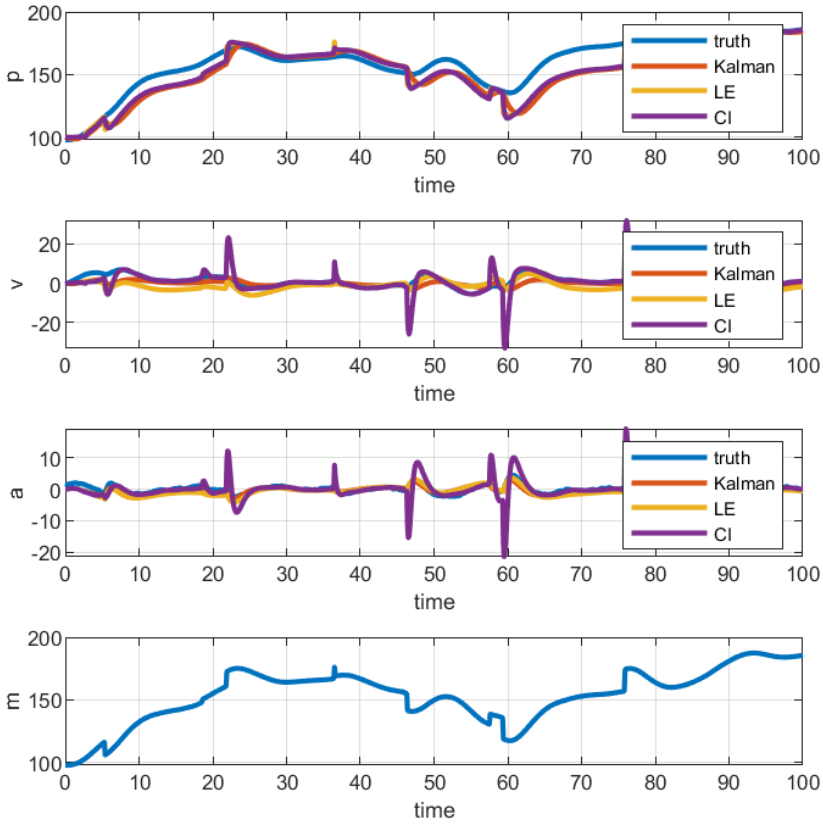

Fig. 1 States, estimates, and measurements for a sample run of the randomly changing disturbance example

Three state estimators are examined: a naïve Kalman filter that treats d as an independent noise source, a largest ellipsoid estimator, and a covariance intersection estimator (which is described in the Appendix). The initial error covariance is $\mathbf{X} = \hat{\mathbf{X}} = diag\,(10, 10, 1)$. The feedback used to form the input is taken from the Kalman estimate.

This example was chosen to showcase the potential benefits of LE estimation. The randomly changing disturbance is not easily handled by state augmentation in a Kalman filter. Figure 2 shows the estimation errors for each of the estimators. The naïve Kalman filter underpredicts the covariance because of the false independent measurement noise assumption. The CI estimator produces extremely conservative estimates of the states that are not directly measured (v and a). The

LE estimator has balanced, consistent performance. This is reinforced by the normalized estimation error squared (NEES) comparison in Fig. 3. NEES is given by $NEES = \tilde{\mathbf{x}}^{\top}\hat{\mathbf{X}}^{-1}\tilde{\mathbf{x}}/dim(\tilde{\mathbf{x}})$, and if the estimator is consistent, should have a mean of 1.

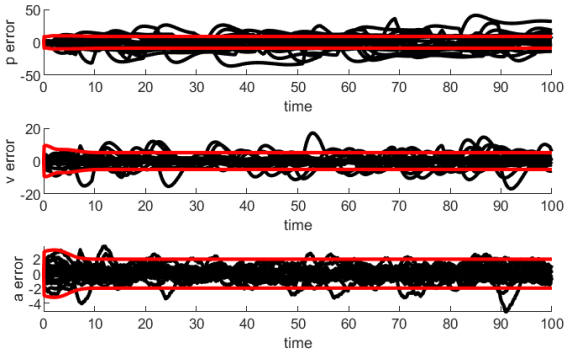

(a) Naïve Kalman filter

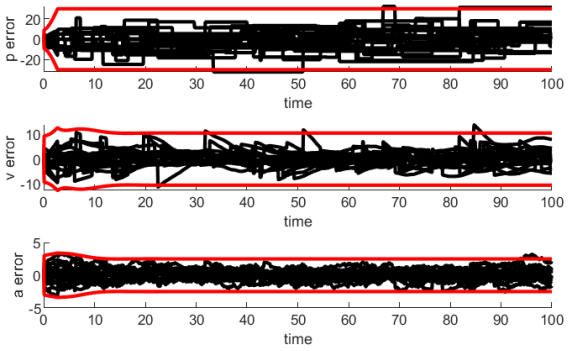

(b) Largest Ellipsoid

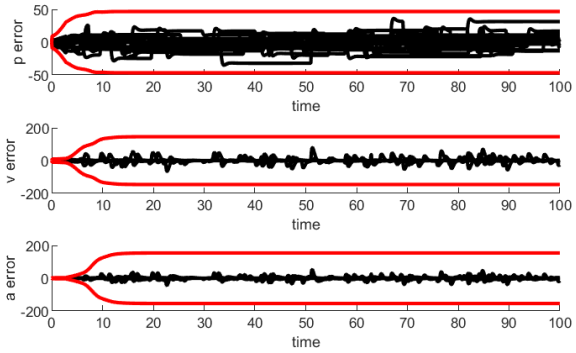

(c) Covariance Intersection

Fig. 2 Estimation errors (black) along with estimator $\pm 3\sigma$ bounds (red)

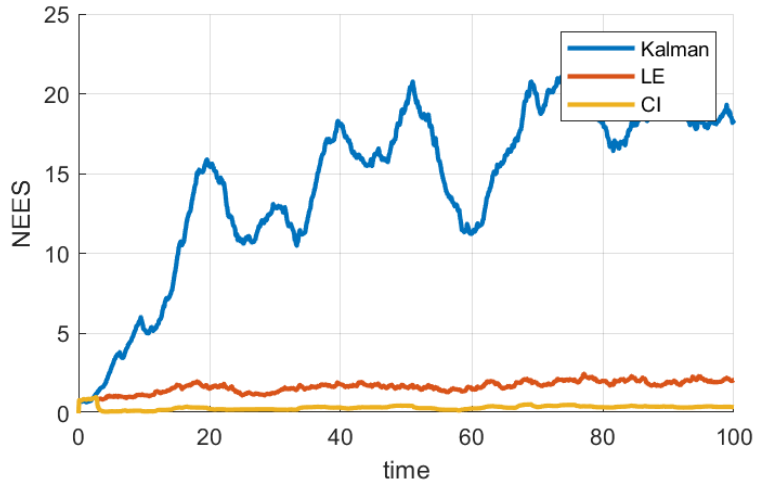

Fig. 3 Average NEES comparison over 20 runs for randomly changing disturbance example

The elements of the LE covariance error are shown in Fig. 4. The solid lines are the elements of $\tilde{\mathbf{X}}_k$ formed by propagating Eqs. 48 and 47, while the dashed lines are the elements of $\tilde{\mathbf{X}}_\infty$ as computed with the approximation that $\hat{\mathbf{X}}_\infty \approx \hat{\mathbf{X}}_k$ for each timestep. The values all converge to 0 or a negative number, which shows that the LE estimator predicted its own trace-consistency.

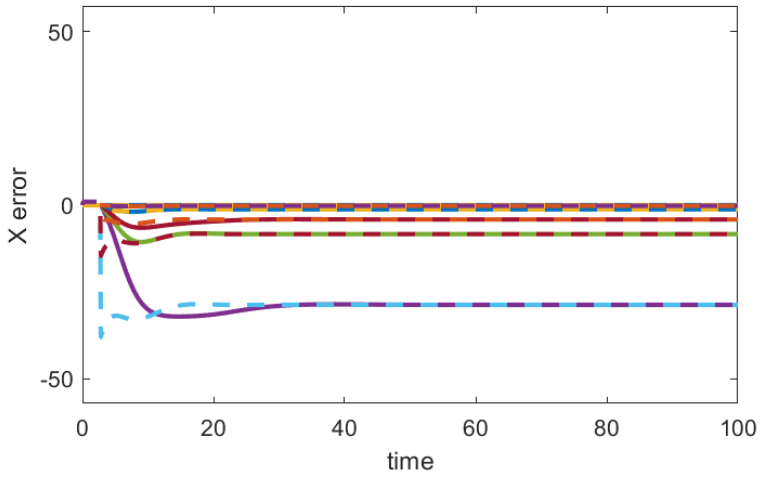

Fig. 4 Elements of the propagated LE covariance error (solid) and the most recent steady-state predictions (dashed)

7. Example: Biased Sinewave Measurements

Consider the state-space model for a randomly driven sine wave with position p, velocity v, and frequency ω:

$$\begin{bmatrix} \dot{p} \\ \dot{v} \end{bmatrix} = \begin{bmatrix} 0 & 1 \\ -\omega^2 & 0 \end{bmatrix} \begin{bmatrix} p \\ v \end{bmatrix} + \begin{bmatrix} 1 & 0 \\ 0 & 1 \end{bmatrix} \begin{bmatrix} w_1 \\ w_2 \end{bmatrix}, \tag{61}$$

where w_1 and w_2 are independent unit white noise processes. The measurement is the position afflicted by a bias:

$$m = \underbrace{\begin{bmatrix} 1 & 0 \end{bmatrix}}_{\mathbf{H}} \underbrace{\begin{bmatrix} p \\ v \end{bmatrix}}_{\mathbf{x}} + \underbrace{\begin{bmatrix} 1 \end{bmatrix}}_{\mathbf{G}} \underbrace{\begin{bmatrix} b \end{bmatrix}}_{\mathbf{y}} \tag{62}$$

As in Section 6, the system is discretized with a timestep of 0.1, and a LE estimator is compared with a naïve Kalman filter and CI estimator.

This example was chosen to break the LE estimator. The average NEES over 20 runs is shown in Fig. 5, with two values of ω. When $\omega = 0.1 \times 2\pi$, the LE estimator is slightly more consistent than the Kalman filter, and the CI estimator is conservative. When ω is changed to $0.5 \times 2\pi$, the LE estimator is less consistent than the naïve Kalman filter. This inconsistency is predicted by the covariance error estimates shown in Fig. 6. As in the previous example, the dashed lines are the elements of $\tilde{\mathbf{X}}_\infty$ as computed with the approximation that $\hat{\mathbf{X}}_\infty \approx \hat{\mathbf{X}}_k$ for each timestep. This metric circumvents the need to propagate $\tilde{\mathbf{X}}_k$ from the beginning and can be used during runtime, although best results are obtained when the estimated $\hat{\mathbf{X}}_k$ has approached its steady-state value. When $\omega = 0.1 \times 2\pi$, all elements of $\tilde{\mathbf{X}}$ are ≤ 0 indicating trace-consistency, while one of them is positive when $\omega = 0.5 \times 2\pi$ indicating the opposite.

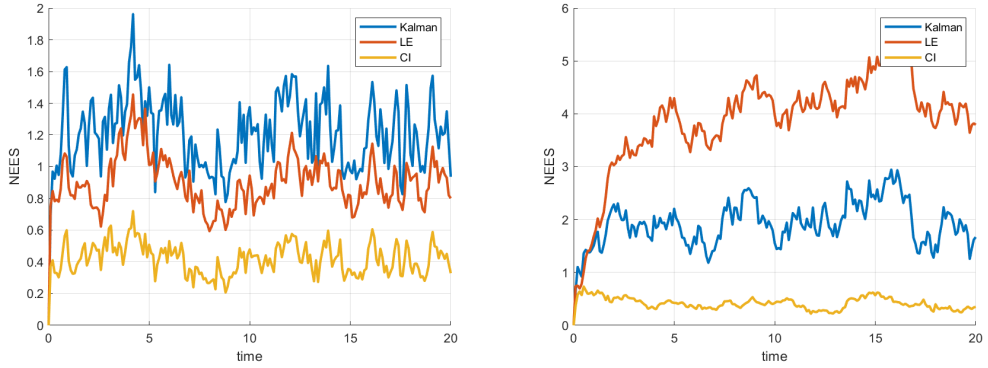

(a) $\omega = 0.1 \times 2\pi$ **(b)** $\omega = 0.5 \times 2\pi$

Fig. 5 NEES comparisons for the biased sinewave example. Changing the ω from $0.1 \times 2\pi$ to $0.5 \times 2\pi$ changes the system enough to cause LE to become inconsistent.

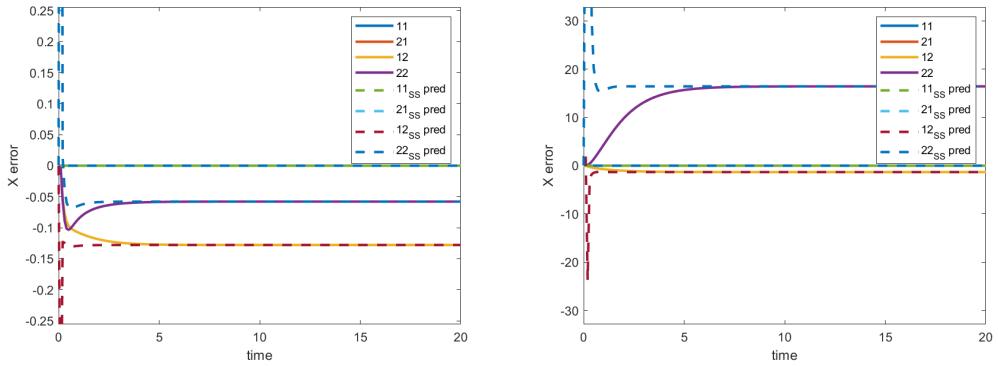

(a) $\omega = 0.1 \times 2\pi$ **(b)** $\omega = 0.5 \times 2\pi$

Fig. 6 Elements of the propagated LE covariance error (solid) and the most recent steady-state predictions (dashed) for the biased sine wave example

8. Conclusions

LE was shown to have a simple formulation and can accurately handle measurement errors that are difficult to model in a Kalman filter. However, it was also demonstrated that the algorithm is not guaranteed to be consistent when the measurement errors are unmodeled biases. The steady-state estimator covariance error can be calculated in this case from the steady-state estimator covariance. Calculating the steady-state LE estimator covariance unfortunately is left as an unsolved problem. The LE estimator covariance at the current timestamp can be used in its place during runtime, and in our examples, this was accurately used to predict estimator consistency.

9. References

1. Schweppe F. Recursive state estimation: Unknown but bounded errors and system inputs. IEEE Transactions on Automatic Control. 1968;13(1):22–28.

2. Witsenhausen H. Sets of possible states of linear systems given perturbed observations. IEEE Transactions on Automatic Control. 1968;13(5):556–558.

3. Gollamudi S, Nagaraj S, Kapoor S, Huang Y. Set-membership state estimation with optimal bounding ellipsoids. In: Proceedings of the international symposium on information theory and its applications; p. 262–265.

4. Calafiore G. Reliable localization using set-valued nonlinear filters. IEEE Transactions on systems, man, and cybernetics-part A: systems and humans. 2005;35(2):189–197.

5. Loukkas N, Martinez JJ, Meslem N. Set-membership observer design based on ellipsoidal invariant sets. IFAC-PapersOnLine. 2017;50(1):6471–6476.

6. Meslem N, Loukkas N, Martínez JJ. A luenberger-like interval observer for a class of uncertain discrete-time systems. In: 2017 11th asian control conference (ascc); p. 2107–2112.

7. Chen B, Hu G. Nonlinear state estimation under bounded noises. Automatica. 2018;98:159–168.

8. Wang Z, Shen X, Zhu Y. Ellipsoidal fusion estimation for multisensor dynamic systems with bounded noises. IEEE Transactions on Automatic Control. 2019;64(11):4725–4732.

9. Chabane SB, Maniu CS, Alamo T, Camacho EF, Dumur D. A new approach for guaranteed ellipsoidal state estimation. IFAC Proceedings Volumes. 2014;47(3):6533–6538.

10. Martinez JJ, Loukkas N, Meslem N. H-infinity set-membership observer design for discrete-time lpv systems. International journal of control. 2020;93(10):2314–2325.

11. Durieu C, Polyak BT, Walter E. Trace versus determinant in ellipsoidal outer-bounding, with application to state estimation. IFAC Proceedings Volumes. 1996;29(1):3975–3980.

12. Liu Y, Zhao Y, Wu F. Ellipsoidal state-bounding-based set-membership estimation for linear system with unknown-but-bounded disturbances. IET Control Theory & Applications. 2016;10(4):431–442.

13. Julier S, Uhlman J. A non-divergent estimation algorithm in the presence of unknown correlations. In: Proc. of the american control conference; Vol. 4; p. 2369 – 2373.

14. Julier SJ, Uhlmann JK. Simultaneous localisation and map building using split covariance intersection. In: Proc. of the ieee/rsj international conference on intelligent robots and systems; p. 1257–62.

15. Leonardos S, Daniilidis K. A game-theoretic approach to robust fusion and kalman filtering under unknown correlations. In: 2017 american control conference (acc); p. 2568–2573.

16. Noack B, Sijs J, Reinhardt M, Hanebeck UD. Decentralized data fusion with inverse covariance intersection. Automatica. 2017;79:35–41.

17. Benaskeur AR. Consistent fusion of correlated data sources. In: Ieee 2002 28th annual conference of the industrial electronics society. iecon 02; Vol. 4; p. 2652–2656.

18. Gustafsson F. Statistical sensor fusion. Studentlitteratur; 2010.

19. Sijs J, Lazar M, Bosch P. State fusion with unknown correlation: Ellipsoidal intersection. In: Proceedings of the 2010 american control conference; p. 3992–3997.

20. Forsling R. Decentralized estimation using conservative information extraction. Linköping University Electronic Press; (vol. 1897).

21. Nygårds J, Deleskog V, Hendeby G. Safe fusion compared to established distributed fusion methods. In: 2016 ieee international conference on multisensor fusion and integration for intelligent systems (mfi); p. 265–271.

22. Sijs J, Lazar M. Empirical case-studies of state fusion via ellipsoidal intersection. In: 14th international conference on information fusion; p. 1–8.

23. Ajgl J, Straka O. On weak points of the ellipsoidal intersection fusion. In: 2017 ieee international conference on multisensor fusion and integration for intelligent systems (mfi); p. 28–33.

24. Noack B, Sijs J, Hanebeck UD. Algebraic analysis of data fusion with ellipsoidal intersection. In: 2016 ieee international conference on multisensor fusion and integration for intelligent systems (mfi); p. 365–370.

25. Bar-Shalom Y, Campo L. The effect of the common process noise on the two-sensor fused-track covariance. IEEE Transactions on aerospace and electronic systems. 1986;(6):803–805.

26. Simon D. Optimal state estimation: Kalman, h infinity, and nonlinear approaches. Wiley-Interscience; 2006.

27. MATLAB release 2019b.

28. Chen L, Arambel PO, Mehra RK. Estimation under unknown correlation: Covariance intersection revisited. IEEE Transactions on Automatic Control. 2002;47(11):1879–1882.

Appendix. Covariance Intersection Estimator

The estimator gain for the CI estimator $\mathbf{K}_k^{CI}$ is derived from the analysis in Chen et al.[28]:

$$\mathbf{K}_k^{CI} = \frac{1}{\alpha_k}\hat{\mathbf{X}}_{k|k-1}^{CI}\mathbf{H}^\top \left(\frac{1}{\alpha_k}\mathbf{H}\hat{\mathbf{X}}_{k|k-1}^{CI}\mathbf{H}^\top + \frac{1}{1-\alpha_k}\mathbf{M}\right)^{-1}.$$

The corresponding covariance update is then

$$\hat{\mathbf{X}}^{CI} = \frac{1}{\alpha_k}\left(\hat{\mathbf{X}}_{k|k-1}^{CI} - \mathbf{K}_k^{CI}\mathbf{H}\hat{\mathbf{X}}_{k|k-1}^{CI}\right).$$

The scalar weight α_k must be optimized at each time step to minimize the trace of $\hat{\mathbf{X}}^{CI}$.

List of Acronyms

CI	covariance intersection
LTI	linear time invariant
NEES	normalized estimation error squared
SVD	singular value decomposition
UBB	unknown but bounded

1 (PDF)	DEFENSE TECHNICAL INFORMATION CTR DTIC OCA
1 (PDF)	DEVCOM ARL FCDD RLD DCI TECH LIB
1 (PDF)	DEVCOM ARL FCDD RLW WE J MALEY